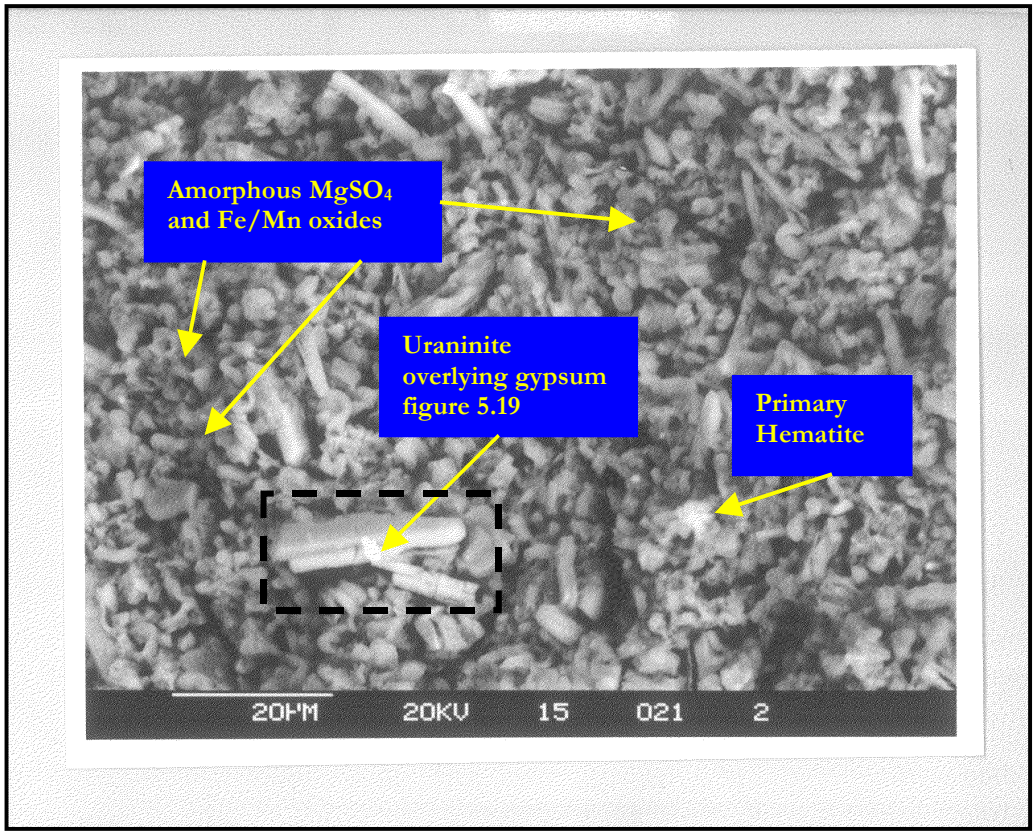

Figure 5.18: SEM field view of primary and authigenic phases, Site 5 (7.11 m) (backscatter mode)

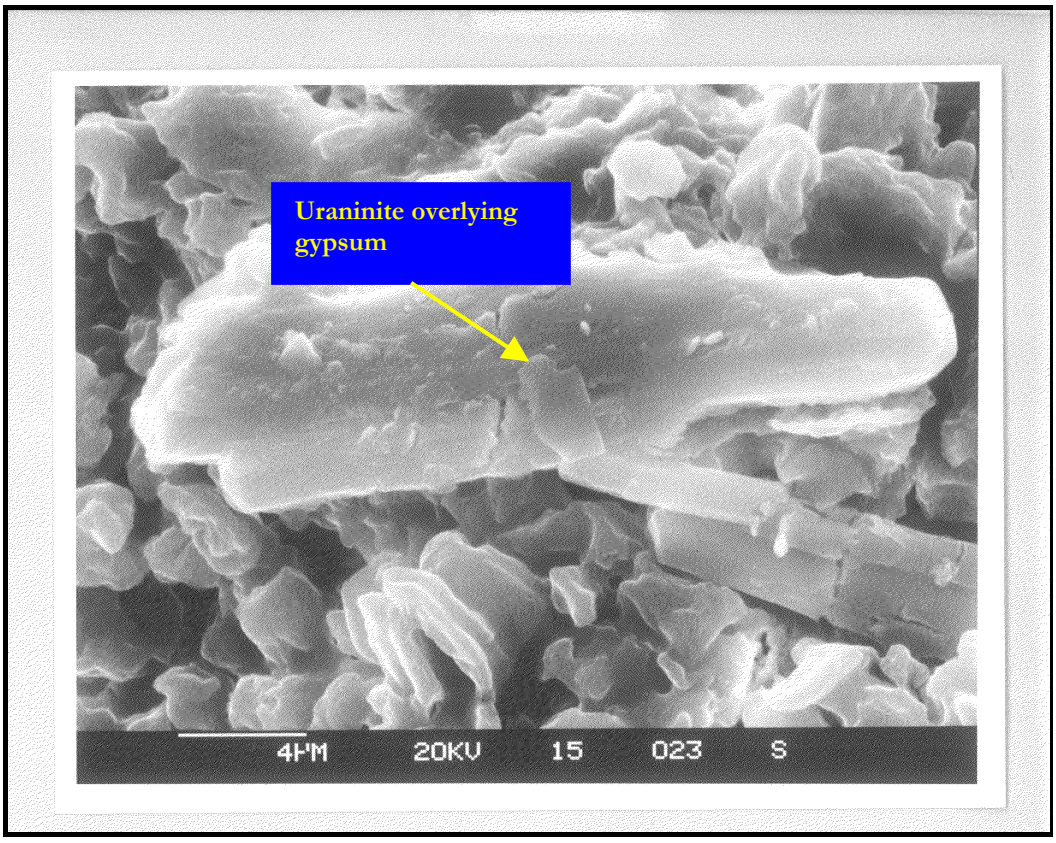

Figure 5.19: Magnified view showing uraninite superimposed on gypsum Site 5 (7.11 m)

Uraninite is the principal primary uranium mineral of the Ranger orebody and is efficiently removed during the milling process. As a consequence, very few particles of uraninite were observed (Figure 5.20) in the tailings during SEM examination. The weathered appearance of uraninite in this image is presumably due to sulfuric acid leaching. Authigenic Fe and Mn oxides are pervasive in the fine tailings fractions often appearing as sub-micron particles.

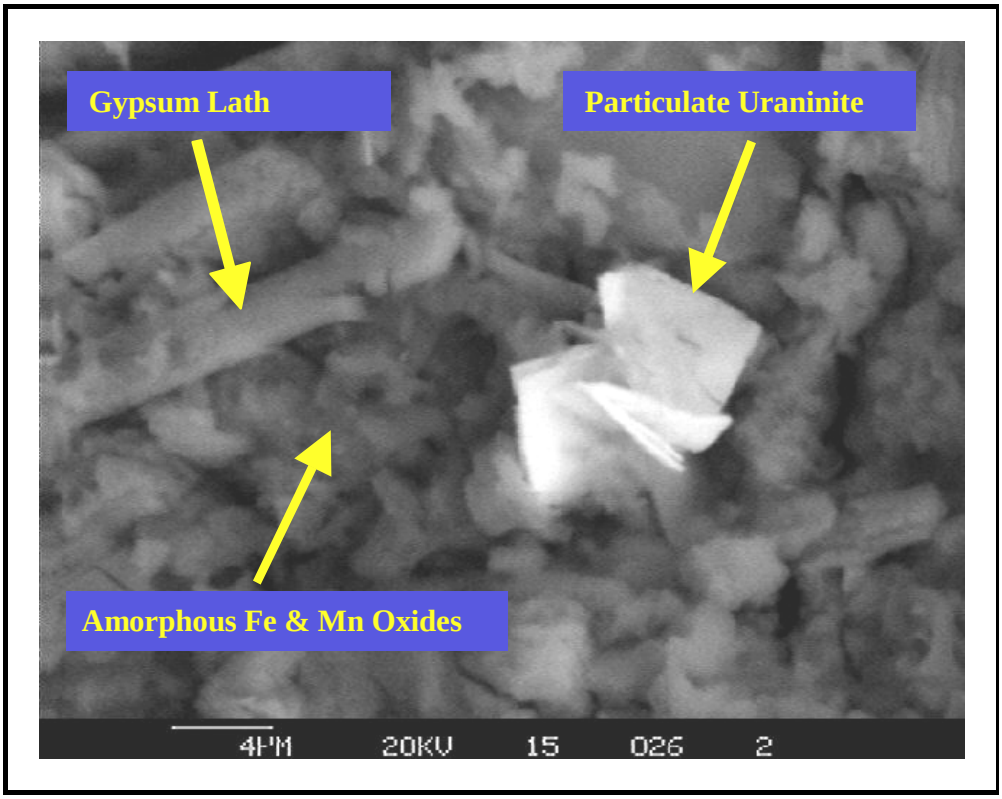

Figure 5.20: Weathered uraninite within a groundmass of amorphous Fe and Mn oxides (backscatter mode)

5.2.2.3 Tailings Geochemistry

A measure of the extent of trace metal enrichment within each sample was obtained by comparing the assay result of each element with the average crustal abundance that has been reported for that element (Levinson, 1974).

Solid phase concentrations of Ba, Zn, Co, Ni and Sr for all tailing types are either near or less than the background ranges observed for crustal rocks (Table 5.5). Uranium, Cu and Pb, however, are enriched in the tailings over crustal abundances by one to two orders of magnitude. With the exception of U, metal concentrations in the coarse tailings are generally lower than the finer grain tailings. As will be shown in the following section, U enrichment in the coarse tailings fraction is due to the residual uranium minerals, brannerite and uraninite.

Table 5.5: Trace metal composition of selected tailings

Tailings Type	Ba mg/kg	Zn mg/kg	Pb mg/kg	Co mg/kg	Cu mg/kg	Ni mg/kg	Sr mg/kg	U mg/kg
Authigenic Phase Site 5, 7.11 m	340	85	1267	30	100	90	29	450
Authigenic Phase Site 5, 11.13 m	258	81	1306	41	533	79	20	748
Fine Grain Site 4, 11.38 m	159	84	1067	21	761	56	58	449
Fine Grain Site 5, 10.34 m	265	66	1327	27	266	69	107	439
Fine Grain Site 6, 12.36 m	278	51	1215	22	321	64	34	348
Coarse Grain Site 6, 5.45 m	78	50	512	21	89	57	16	421
Crustal Abundance	425	165	12.5	25	55	75	375	2.7

In mineralised areas such as the Alligator Rivers uranium province, it is not uncommon to find a range of metals enriched in excess of crustal abundances. Furthermore, this enrichment does not necessarily signify an environmental risk as the issue is not the total concentrations of contained metals/radionuclides in the tailings, but rather their bioavailability and potential for mobilisation and subsequent release at levels considered to be toxic to human health and the environment. It is thus important to define and understand the solid state speciation of metals and radionuclides in the tailings. The following section discusses the phase distribution of metals/radionuclides within the tailings.

5.3. Solid State Speciation

When attempting to model the long term behaviour of the radionuclides and their interactions with porewater, it is important to know their geochemical form or bonding within the tailings. One method widely used for this purpose is sequential extraction, whereby a series of solvents of increasing activity are used to determine the chemical association of heavy metals and

radionuclides with specific solid phases in soils and sediments (Tessier et al. 1979; Yanase et al. 1991; Suksi et al. 1996). The chemical speciation arrived at for these materials are used as a criterion of their potential for biological uptake and remobilisation into the aqueous phase.

The main geochemical phases within the tailings (as described in Section 5.1.1) that have the potential to control the solid state speciation of metals and radionuclides include:

- Evaporites ($MgSO_4 \cdot xH_2O$, $CaSO_4 \cdot xH_2O$)
- Exchangeable and carbonate phases
- Amorphous minerals such as oxides of Al, Fe and Mn
- Crystalline iron oxides
- Primary and secondary U minerals
- Sulfate precipitates (barite, jarosite)
- Phyllosilicates and/or other clay fractions
- Resistate minerals (quartz, muscovite)

As previously described in Chapter 3 (see Table 3.2), a six step sequential extraction procedure was used to selectively dissolve the various mineral assemblages. Samples selected for the sequential extraction procedure are summarised in Table 5.6.

Table 5.6: Sequential extraction samples

Sample Site	Depth (m)	Description	Code
5	7.11	Authigenic FeO_x MnO_x and gypsum phases	Gel Phase
5	10.34	Predominantly fine grain (silt) lithogenic tailings	Fine Tailing
6	5.45	Coarse grain (sand) lithogenic tailings with interbedded fine grain tailings	Coarse Tailing

5.3.1 Phase Selectivity and Mass Recovery

The validity of this technique to assess the speciation of radionuclides and trace metals is primarily dependent on the ability of the various extraction reagents to selectively target their respective mineralogical phases.

Two methods were used to verify this important performance criterion: (1) the use of differential XRD to detect changes in mineralogical composition in the tailings sample before and after each chemical treatment and (2) measurement of dissolved indicator species such as Al, Fe, Mn, Si and Ca following each successive treatment.

Figures 5.21 and 5.22 show the results of the differential XRD scans that were typical of the tailings samples following successive chemical treatments. The scans clearly show that despite the presence of up to 14% gypsum in the tailings samples, the initial water treatment effectively solubilised this phase and removed it from the solids fraction. Hence, there was little to no gypsum carry-over in successive chemical treatments.

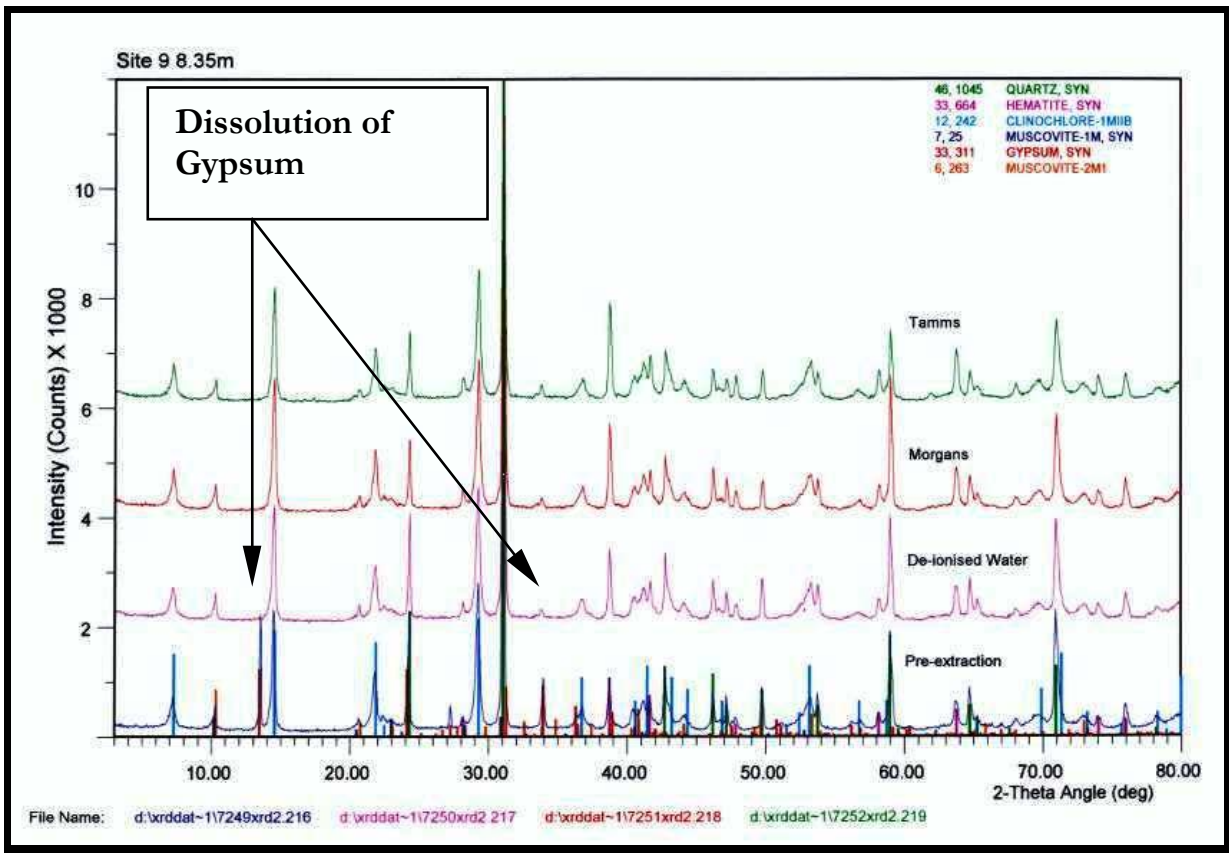

Figure 5.21: Differential XRD scan of fine tailings (Site 5 at 10.3 m) following water, exchangeable and acid soluble extractants

Following the water treatment, there was no measured mineralogical change in the tailings samples until the crystalline iron extractant (CBD) was introduced. This result is not surprising as the abundance of carbonate minerals that would normally be extracted by Morgan's solution (as exchangeable phases) is low and below the detection limit of XRD. Similarly, amorphous Fe and Mn oxides while pervasive are not detected by XRD. These phases were measured as solubilised products in the leachate.

Hematite degradation was observed (Figure 5.22) following the addition of CBD however it is suspected that there was some carry over into the alkaline earth and possibly the clay mineral phase extractions. This assumption is predicated on the mass distribution of Fe in the tailings samples and the presence of known iron bearing minerals such as Mg-chlorite and hematite.

The addition of 6 M HCl to dissolve clay minerals was highly selective with complete removal of chlorite. Resistate minerals such as quartz and muscovite are geochemically stable and were unaffected by the addition of 6 M HCl.

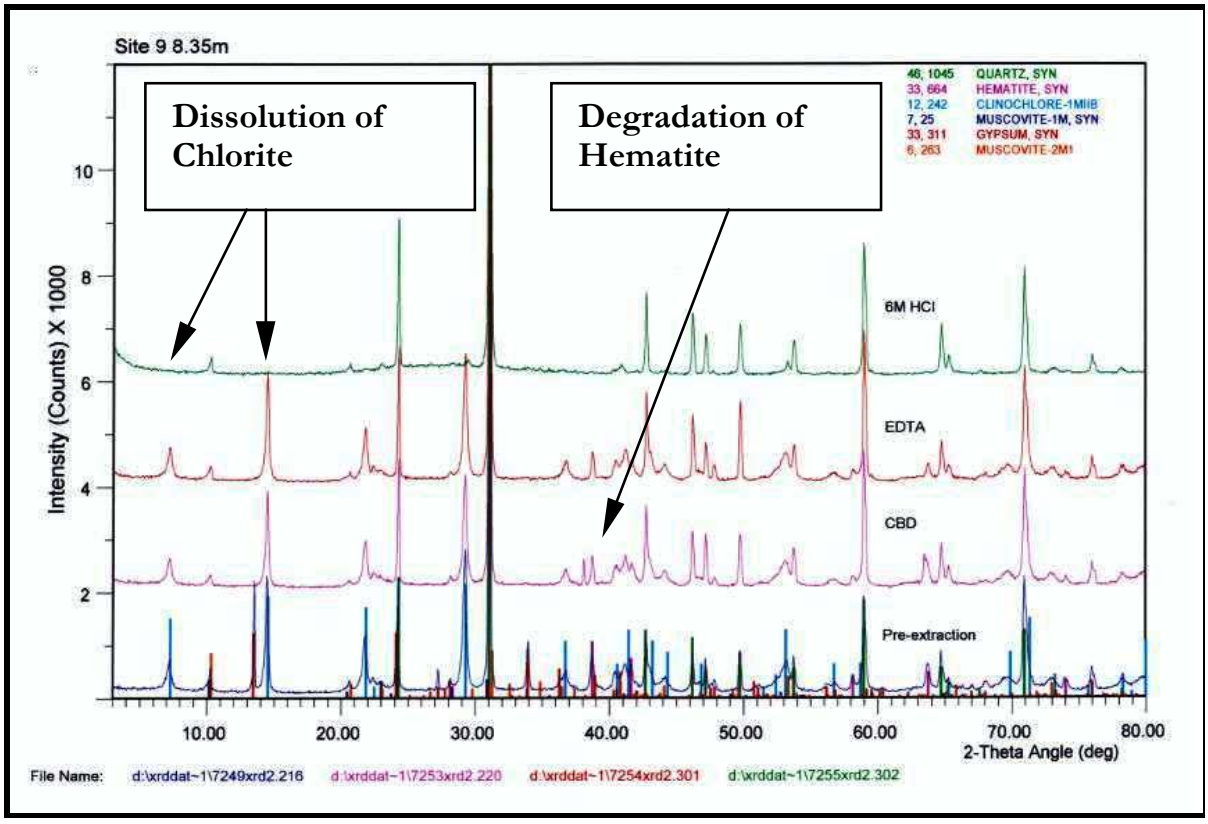

Figure 5.22: Differential XRD scan of fine tailings (Site 5 at 10.3 m) following crystalline Fe, alkaline earth and residue extractants

Although differential XRD provides a convenient method to assess extractant selectivity for major mineral phases it is somewhat limited when applying the technique to trace (< 5% wt/wt) mineral assemblages such as uranium and amorphous phases. Furthermore, interpretation of results (McCarty et al. 1998) can also be impacted by:

- The relative differences in preferred orientation between the phases in the treated and untreated diffraction scans;
- The possible crystallisation of new solid compounds resulting from the treatment;
- Sample heterogeneity; and
- Partial chemical dissolution of solid phases, such as quartz that is thought to be resistant to the treatment. Interpretive errors can arise if the quartz is used as an internal standard.

For this reason, a suite of geochemical phase indicators (Al, Fe, Mn, Si and Ca) were also measured in both the extracted tailings solids and leachate recovered from successive chemical treatments.

The partitioning of these indicator elements for each of the gel, fine grain and coarse grain tailings are shown in Figures 5.23, 5.24 and 5.25, respectively. Mass recoveries for each element studied (Table 5.7) were all within ±10% of the total concentration measured in the pre-extracted tailings solids.

Elemental fractionation determined by sequential extraction shows that the majority of calcium contained in the tailings solids is either water soluble or exchangeable. Around 10% of the total manganese is also partitioned between the water soluble and exchangeable phases, indicating the relative mobility of this metal in the tailings pile.

In the gel and fine grain tailings (Figures 5.23 and 5.24), in excess of 20% of the total manganese, iron and aluminium were extracted by Tamm's acid oxalate which indicates the presence of amorphous metal oxyhydroxides or readily reducible phases. With the exception of manganese (15% mass extracted), negligible quantities of amorphous minerals were extracted from the coarse grain tailings (Figure 5.25). Crystalline iron, presumably primary hematite, is present in the gel, fine grain and coarse grain tailings with extraction recoveries of 6, 9 and 12%, respectively, being observed.

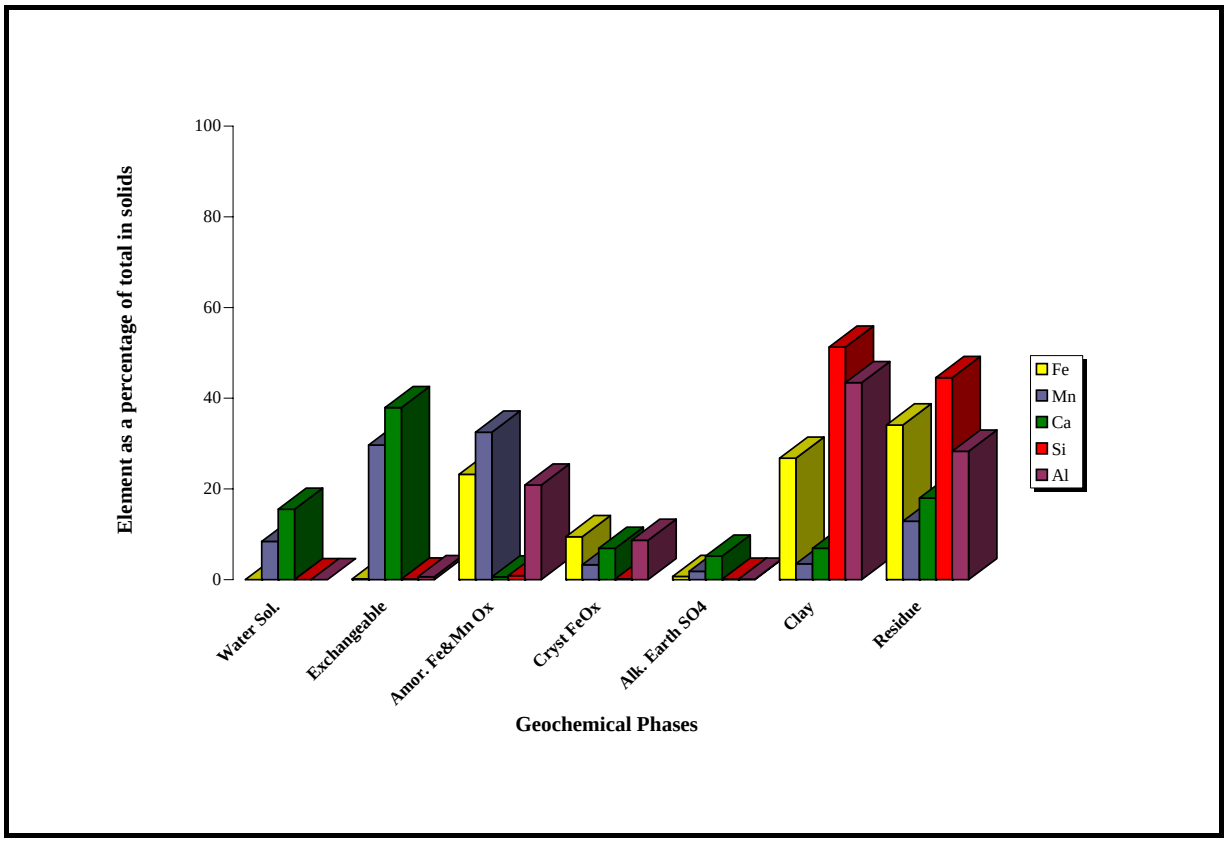

Figure 5.23: Elemental fractionation Site 5 (7.11 m) – gel fraction

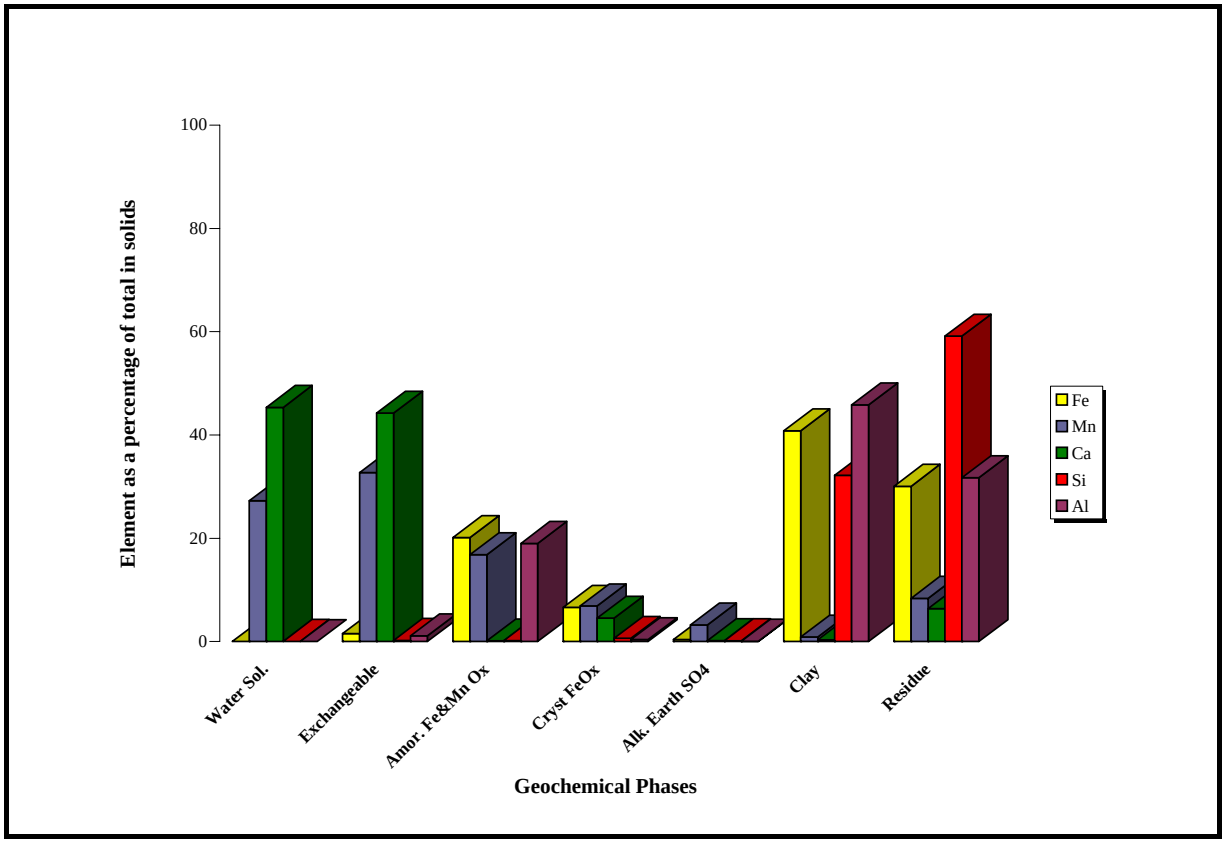

Figure 5.24: Elemental fractionation Site 5 (10.34 m) – fine grain tailings

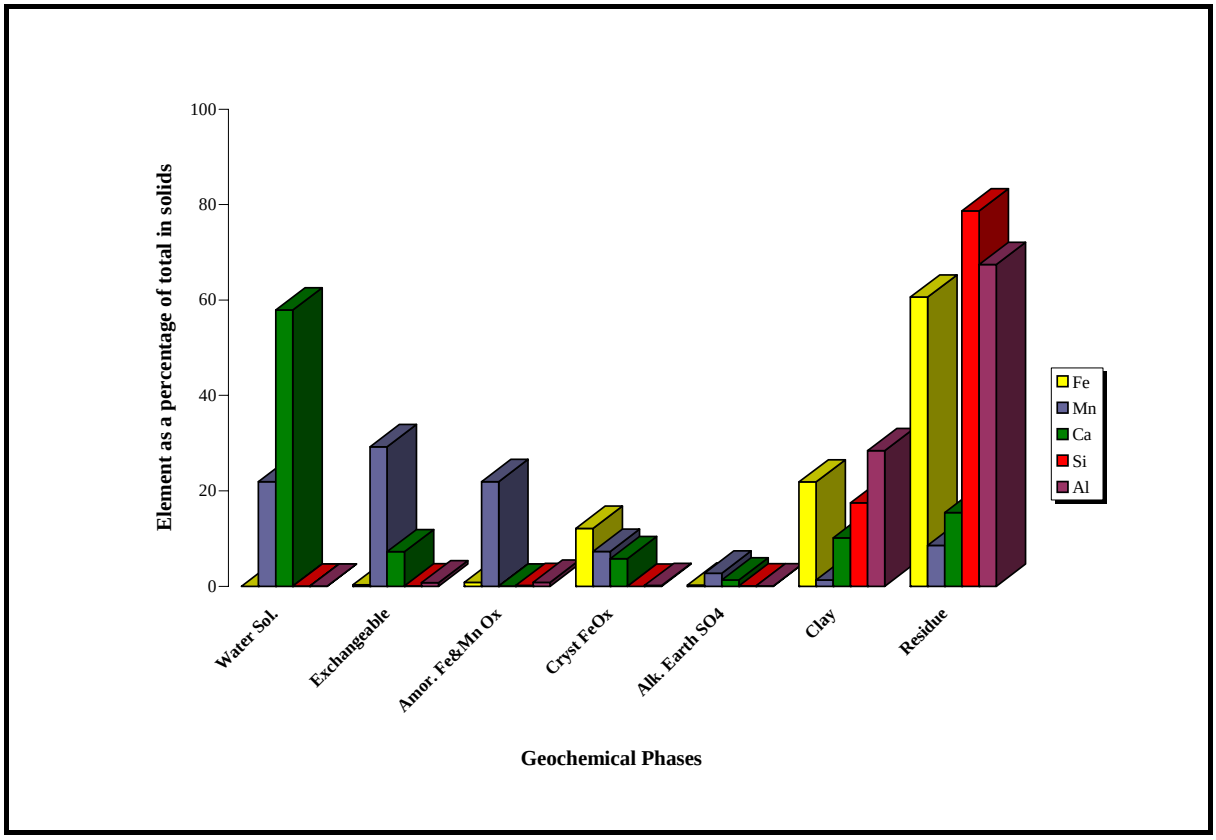

Figure 5.25: Elemental fractionation Site 6 (5.45 m) – coarse grain tailings

The addition of 6 M HCl extracted between 30 to 40% of the total aluminium, iron and silica in the gel/fine grain tailings, which is consistent with the dissolution of Mg-rich chlorite and Fe bearing aluminosilicates. The relative recoveries decreased to around 20% in the coarse grain tailings, which is not surprising as quartz is the dominant mineral for this tailings size fraction (see Figures 5.8 and 5.9).

The residue fraction comprises of quartz and muscovite that are not affected by the 6 M HCl extraction. The abundance of these two minerals in the residue fraction explains the magnitude of measured aluminium and silica. The solid phase Fe concentrations are also attributed to muscovite as Fe can act as an isomorphous substitute for Al. Iron oxide concentrations as high as 2.1% were measured in muscovite for tailings collected at Site 4 (see Table 5.4). This result is consistent with those reported by Deer et al. (1966) in which FeO concentrations in muscovites typically varied between 2 and 4 percent.

In contrast, the relatively high concentrations of calcium and manganese are anomalous. These are possibly present as isomorphous replacements within muscovite (Deer et al. 1966) or an

artifact of experimental errors associated with extraction end points and quantification of elemental mass recoveries.

Table 5.7: Mass recovery of elements constituting key geochemical phases

Parameter	Extracted Phase	Elemental Mass		
		Gel Phase	Fine Tailings	Coarse Tailings
Al (mg)	Pre-extracted solids	576	589	387
	Total mass extracted by successive treatments	424	391	117
	Mass remaining in residue	163	187	261
	% Mass Recovery	101	98	98
Fe (mg)	Pre-extracted solids	560	392	824
	Total mass extracted by successive treatments	338	273	291
	Mass remaining in residue	191	118	499
	% Mass Recovery	94	100	96
Mn (mg)	Pre-extracted solids	16	102	27
	Total mass extracted by successive treatments	12.7	77	7.4
	Mass remaining in residue	2.1	22	18
	% Mass Recovery	92	97	93
Si (mg)	Pre-extracted solids	1561	1243	2002
	Total mass extracted by successive treatments	821	416	355
	Mass remaining in residue	695	735	1575
	% Mass Recovery	97	93	96
Ca (mg)	Pre-extracted solids	29	219	69
	Total mass extracted by successive treatments	21	191	41
	Mass remaining in residue	5.2	30	26
	% Mass Recovery	91	101	98
U (µg)	Pre-extracted solids	2241	7346	5990
	Total mass extracted by successive treatments	1523	5829	3300
	Mass remaining in residue	574	1222	2557
	% Mass Recovery	94	96	98
Ra (Bq)	Pre-extracted solids	260	180	250
	Total mass extracted by successive treatments	213	128	177
	Mass remaining in residue	57	61	70
	% Mass Recovery	104	105	99

5.3.2 Uranium and Radium Trends in Geochemically Defined Phases

Figures 5.26 and 5.27 show the phase distribution of uranium and radium for tailings samples representative of authigenic or "gel" phases (Site 5, 7.11m), fine grain tailings (Site 5, 10.34 m) and coarse grain tailings (Site 6, 5.45 m).

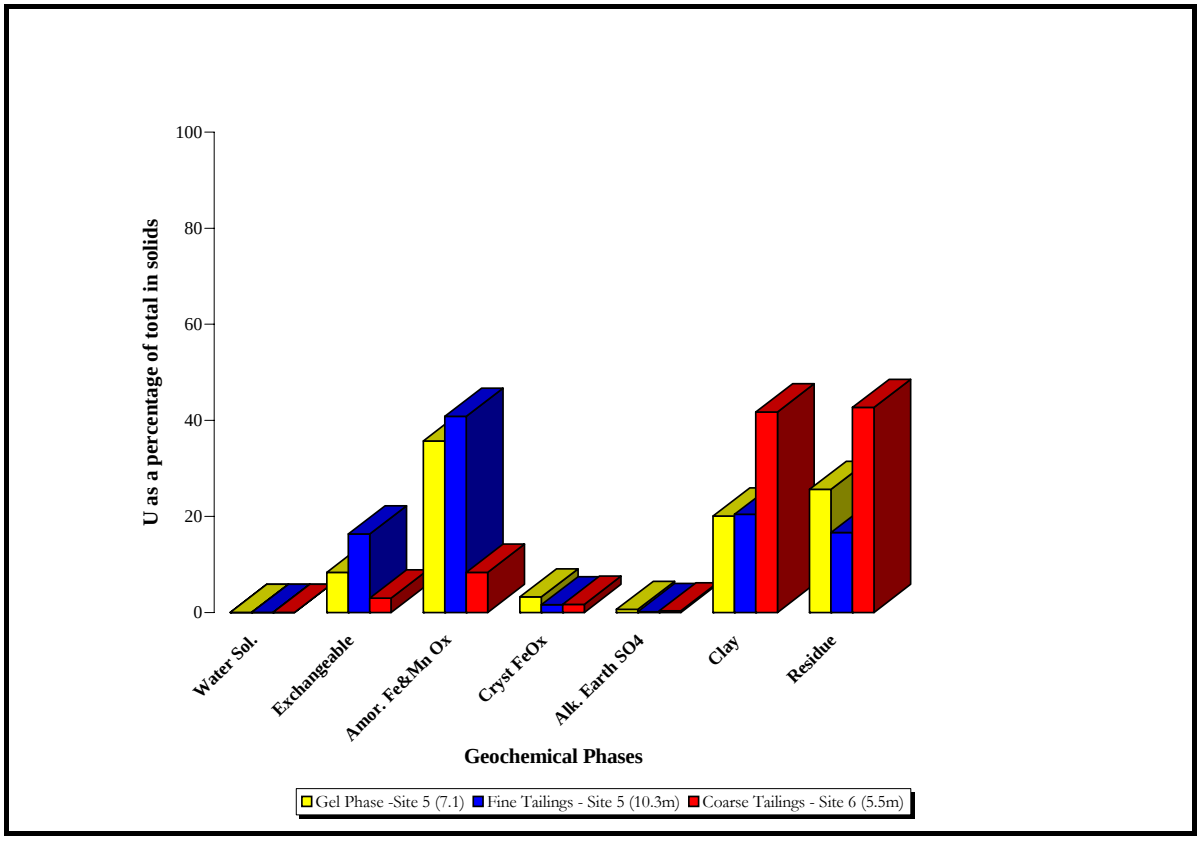

Figure 5.26: Uranium partitioning among geochemical phases

The phase distribution of uranium between the three size fractions is striking. For the coarse tailings, around 30% of the total uranium was extracted by 6 M HCl which is indicative of the dissolution of primary uranium minerals associated with the host rock chlorite. A similar amount of uranium was also measured in the residue fraction. Based on SEM examination this form of uranium is believed to be brannerite (UTi_2O_6) (Figure 5.27). Brannerite is a highly refractory oxide that is relatively insoluble (even in acidic environments) and unlikely to be remobilised within the tailings pile.

The remaining uranium was either extracted as an exchangeable fraction (3%) or associated with amorphous and crystalline iron oxides, 8 and 2% respectively.

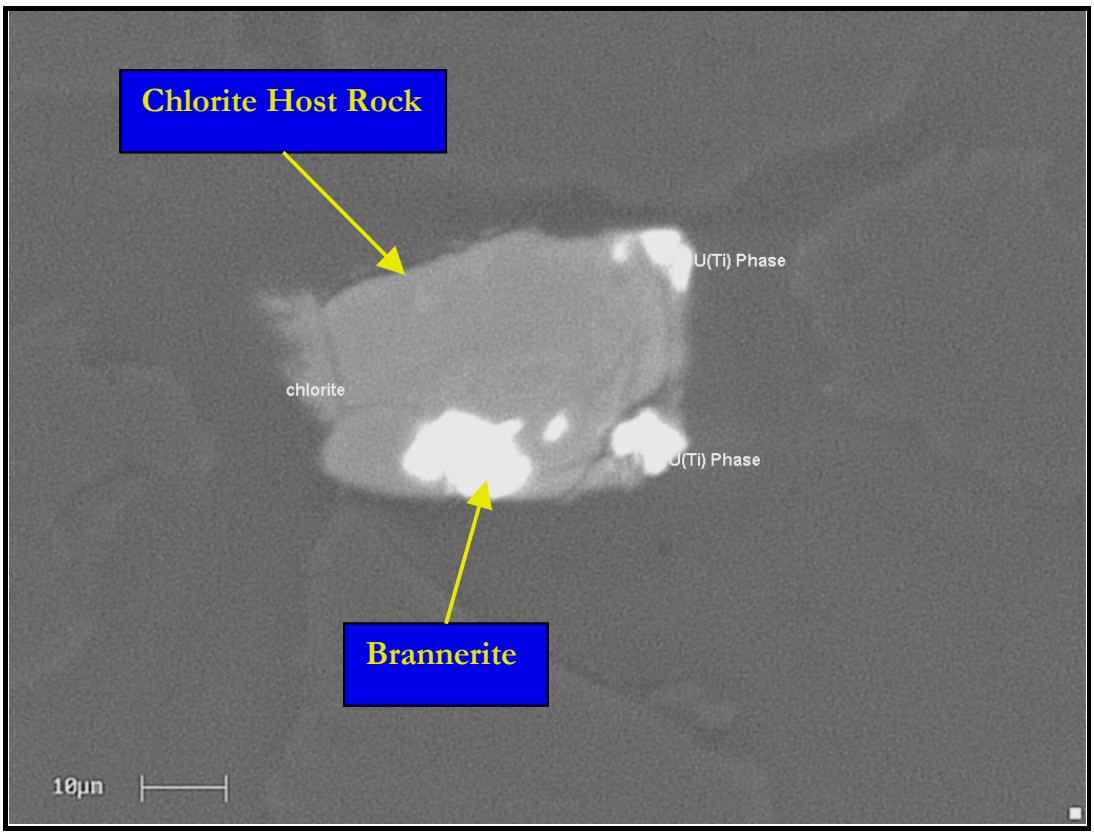

Figure 5.27: SEM image of coarse grain tailings showing refractory brannerite in association with Mg – chlorite (back scatter mode)

In contrast, uranium contained in the gel and fine grain tailings was predominantly extracted with the Morgan's (8 to 16%) and Tamm's acid oxalate (35 to 40%) solutions, suggesting an occurrence with exchangeable phases and hydrous oxides of iron and manganese respectively. Uranium associated with the ion exchangeable phases is in a highly labile form and accessible to underlying aquifers via tailings seepage.

Uranium contained in the Tamm's acid oxalate fraction is either adsorbed onto the surfaces of iron and manganese hydrous oxides or present as secondary uranium minerals such as saleeite ($Mg(UO_2)_2(PO_4)_2 \cdot 8H_2O$), sklodowskite ($Mg(UO_2)_2Si_2O_7 \cdot 6H_2O$) and schoepite ($UO_3 \cdot 2H_2O$), (Yanase et al. 1991). These minerals and oxide phases are relatively stable in the prevailing geochemical environment and even if the latter phases were to undergo enzymatic reduction by heterotrophic bacteria, studies by Lovely et al. (1993) show that dissimilatory processes would also reduce soluble U(VI) to insoluble U(IV). Evidence for such processes is provided in the following sections and Chapter 6.

Like uranium in the gel and fine grain tailings, the partitioning of radium (Figure 5.28) is mainly between the ion exchangeable phase and readily acid soluble phases. The most labile

form is exhibited by the coarse grain tailings with around 50% of the available radium being associated with the exchangeable phase. These findings are consistent with studies by Benes et al. (1981) and Landa and Bush (1990), which demonstrate that radium is mobilised from the ore during the sulfuric acid leach process but is then rapidly removed from solution by sorption onto clays and organic matter. This translocation or phase redistribution results in a more loosely bound or labile form that is potentially accessible for release to underlying aquifers.

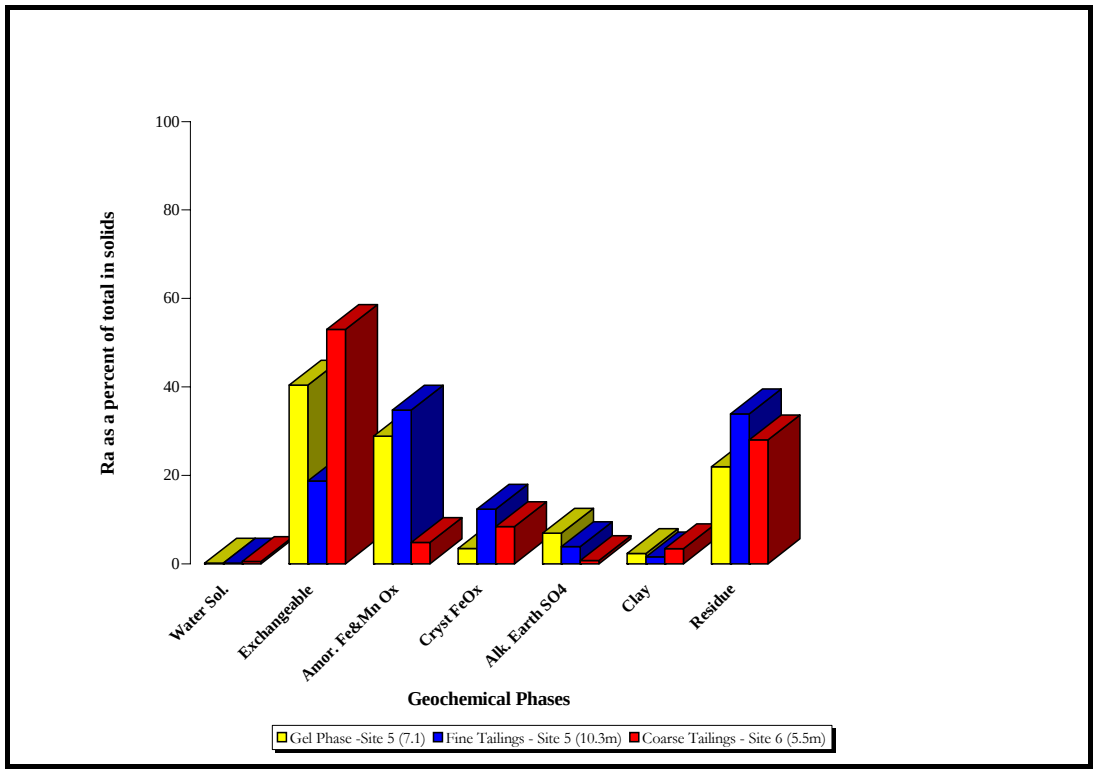

Figure 5.28: Radium partitioning among geochemical phases

The mechanism by which the initial sorption of radium by clays occurs in the sulfuric acid leaching circuit of the mill is not entirely understood (Landa and Bush, 1990). Benes (1982) indicates that in typical sulfuric acid circuits about 70-98% of the dissolved radium occurs as a complex ion pair ($RaSO_4^0$), which implies that sorption in the tailings, is initially achieved via a non-electrostatic bond.

Following lime neutralisation (pH > 6), the predominance of the $RaSO_4^0$ species decreases in favour of the divalent cation, Ra^{2+} (Levins et al. 1978). Under this geochemical environment, Levins et al. (1978) showed that this form of labile radium either co-precipitates or adsorbs onto precipitating manganese and iron hydrous oxides. The findings of this study are consistent

with those of Levins et al. (1978) in which 35 to 40% of the available radium in the gel/fine grain tailings (Figure 5.28) was extracted with the hydrous iron and manganese phases.

The tendency for radium to co-precipitate with divalent sulfate salts is well documented (Benes, 1984; Snodgrass and Hileman, 1985; Paige et al. 1998) and suggests that dissolution of a radium/barium sulfate co-precipitate may control much of the radium found in tailings. Studies by Ritcey (1990) also found that radium could be associated with the sulfate minerals barite ($BaSO_4$), celestine formerly known as celestite ($SrSO_4$), anglesite ($PbSO_4$), jarosite ($KFe_3(SO_4)_2 \bullet 6H_2O$) and gypsum ($CaSO_4 \bullet 2H_2O$).

To evaluate this hypothesis, alkaline EDTA was included in the sequential extraction scheme to selectively dissolve alkaline earth sulfate phases. As shown in Figure 5.28, only a relatively small percentage (≈ 7%) of the total radium was associated with the EDTA extraction step despite the common occurrence of micro-crystalline barite (Figure 5.17). Phase selectivity errors are unlikely as apart from 6 M HCl which follows the EDTA step, barite is relatively insoluble in the other extractants (Benes et al. 1981).

The observed trends may in part be explained by the 100-fold decrease in sulfate concentration as gypsum precipitates upon neutralisation, leading to dissolution of radium (in accordance with the common ion effect) which is quickly and extensively co-precipitated/adsorbed by iron and manganese hydrous oxides. While the initial formation of alkaline earth sulfates appears to be inhibited they may tend to form upon ageing in the tailings pile. Large scale column studies (Chapter 6) were conducted to assess the long term leachability of both labile radium and uranium.

Sequential extraction procedures in general do not have clearly defined endpoints and the amounts of any species extracted are technique dependent. With complex, heterogeneous solids such as tailings the technique appears mainly useful in comparing the relative extractions of radionuclides/metals from different tailings/ores under standardised extraction conditions. Within this limitation, the technique has the potential to provide useful information on the potential mobility of radionuclides and on their geochemical form within the tailings.

5.4. Chemical Manifestations of Dissolved Radionuclides and Metals in the Tailings Pond and Underlying Porewaters

Upon their deposition, tailings porewaters are little more than pond (process) water trapped between tailings particles and in the absence of chemical reactions, the composition of porewaters would be identical to the overlying tailings pond water. In time however the porewaters evolve in accordance with various biogeochemical processes that occur at the mineral water interface.

To properly interpret the various diagenetic processes that govern the observed radionuclide/trace metal porewater profiles in the tailings pile, it is necessary to understand the mechanisms which control their mobility and partitioning between the solid phase and porewater. Studies by Lovley et al. (1993) and Abdelouas et al. (1998) showed that the microbially mediated oxidation of organic matter coupled with the reduction of Fe(III), Mn(IV) or U(VI) has a profound affect on the inorganic geochemistry of naturally occurring marine sediments.

To assess whether these mechanisms are governing the observed porewater trends, relevant data were examined from four perspectives: 1) tailings pond water; 2) major ion chemistry; 3) redox chemistry and 4) radionuclide/metal mobility.

5.4.1 Chemistry of the Tailings Pond Water

The tailings pond water is characterised by a near neutral to slightly acidic pH (Figure 5.29) with high conductances in the order of 10 to 25 mS/cm (Figure 5.30). Magnesium, which is liberated from the dissolution of chlorite, and SO_4 are the major ionic species contributing to the observed electrical conductance (Figures 5.30 and 5.31). Within the tailings pond water, $MgSO_4$ is highly soluble and unlike sparingly soluble gypsum, the equilibrium concentrations of magnesium and sulfate are largely controlled by the cyclical effects of wet season dilution and dry season evapoconcentration. In contrast, calcium concentration trends (Figure 5.32), while showing signs of cyclical climatic effects, are relatively stable, ranging between 300 to 500 mg/L. Calcium solubility is presumably controlled by the formation of gypsum as either an authigenic phase in the dam or as a secondary phase following lime neutralisation.

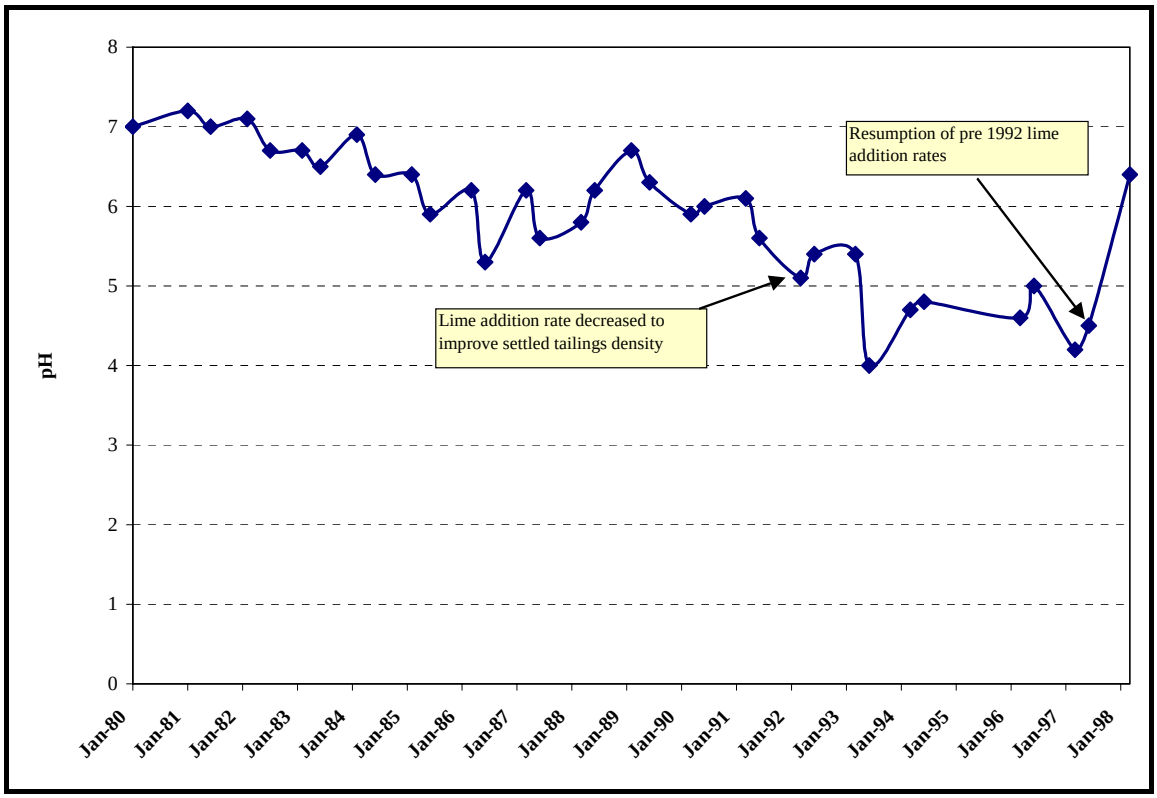

Figure 5.29: Tailings pond water pH trends

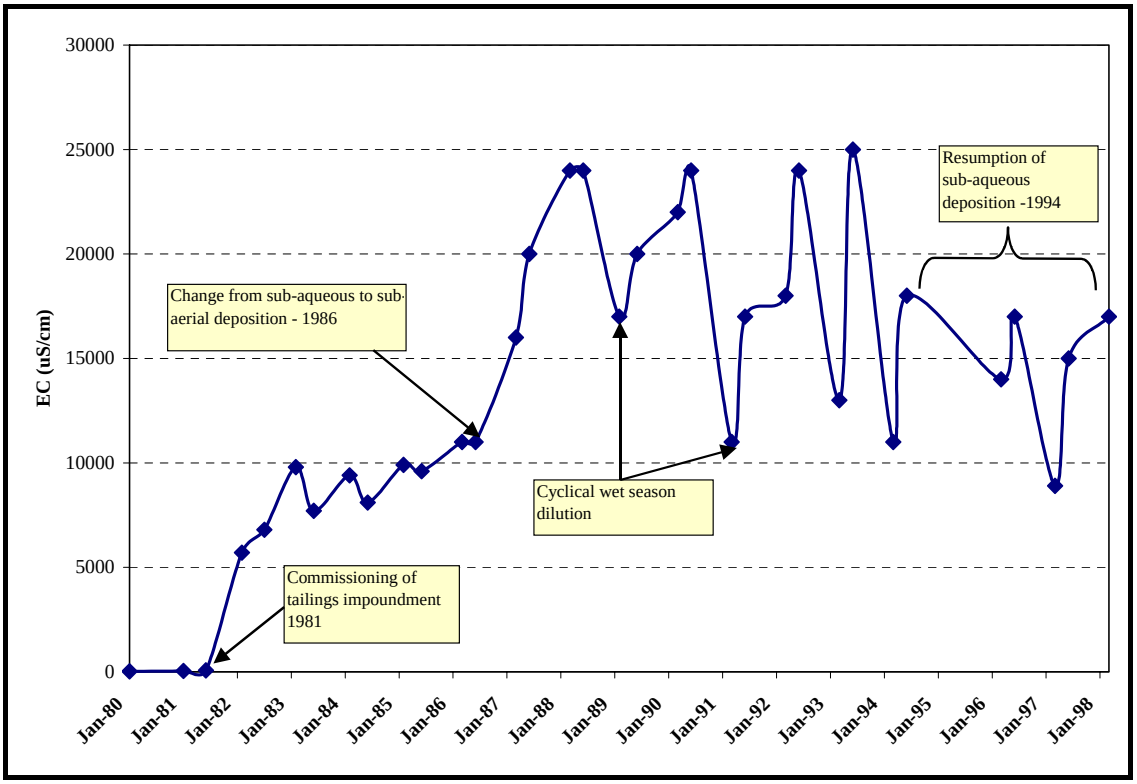

Figure 5.30: Tailings pond water electrical conductivity trends

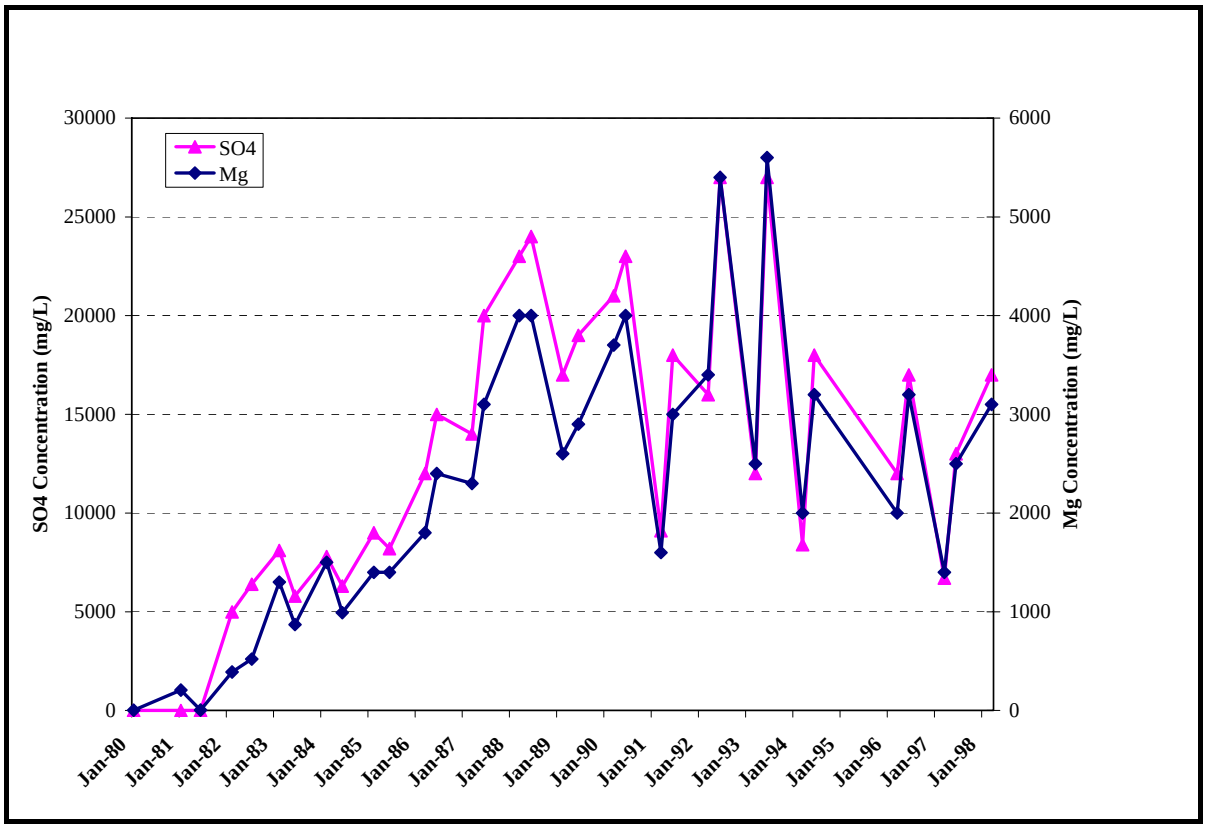

Figure 5.31: Dominant dissolved ions in tailings pond water

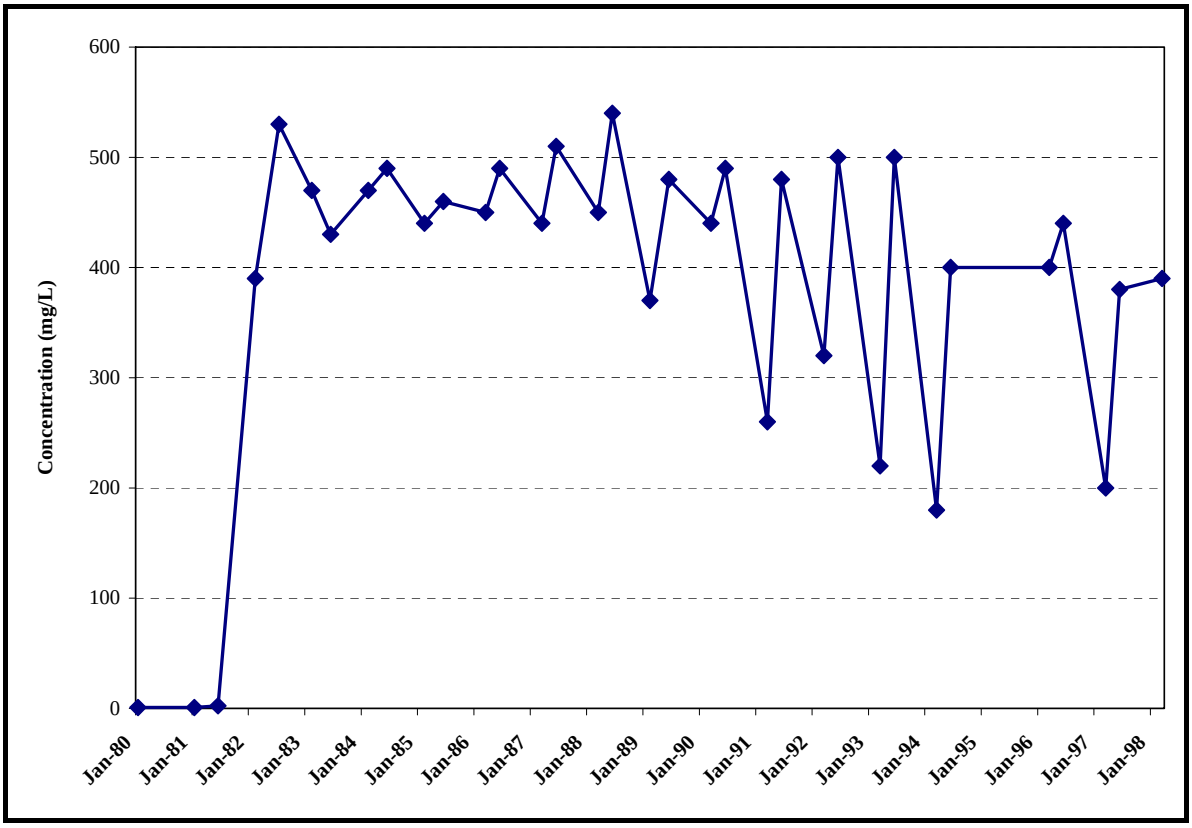

Figure 5.32: Tailings pond water calcium trends

Tailings depositional practices also have a profound effect on water chemistry, where a discrete and significant increase in conductance was observed following the transition from sub-aqueous to sub-aerial deposition in 1986. At the time of transition, the tailings were at RL 35. This depth is significant as tailings porewater and geochemical anomalies, discussed in the following sections, coincide with the transition from sub-aqueous to sub-aerial deposition.

The primary objective of changing to sub-aerial deposition was to increase the settled density of the discharged tailings from around 0.8 t/m^3 (sub-aqueous basis) to 1.2 t/m^3 by establishing beaches around the perimeter of the impoundment. Beach establishment was augmented by improved water management practices that maximised the use/return of tailings water to the processing plant. The pH of the tailings slurry was also reduced from > 7 to < 6 to inhibit the formation of low density floc. These three management practices resulted in a concomitant increase in the tailings solids to pond water ratio and a 2.5 fold concentration increase in dissolved solids (Figure 5.31).

Tailings deposition in the dam ceased in 1995/6 following the commissioning of Pit #1 as a tailings repository. The dam is now used to evaporate excess process/tailings water and as such there is a permanent water cover over the tailings solids.

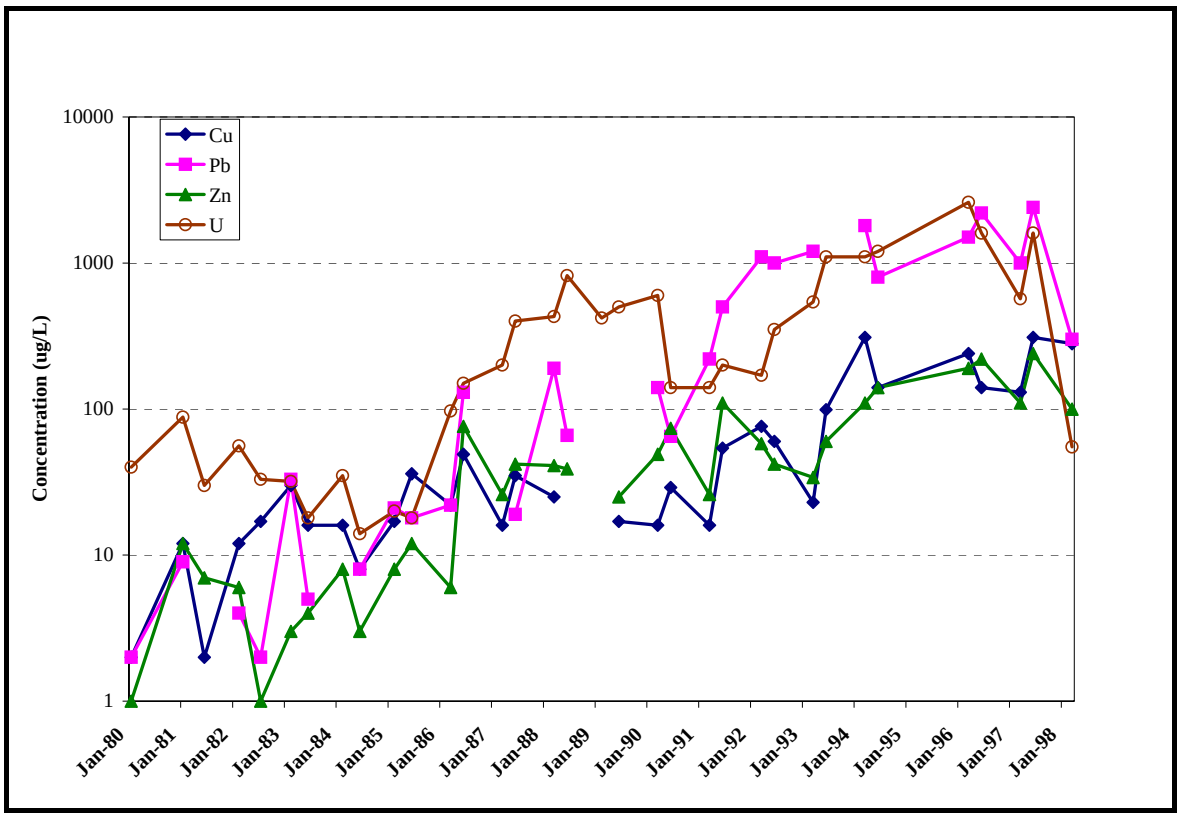

Figure 5.33: Tailings pond water trace metal trends

Trace metal concentrations (Figure 5.33) also significantly increased (1 to 2 orders of magnitude) following the introduction of subaerial deposition. In contrast to the major ions (SO_4 and Mg) the concentration increase for the trace metals is far greater than can be attributed to evapoconcentration alone, thus other geochemical processes such as sulfide oxidation must be contributing to the dissolved metal burden.

Based on the historical pond (surface) water quality data, there is sufficient evidence to suggest that the geochemical mechanisms governing solute mass transfer and metal reactivity differed markedly between the subaqueous and subaerial sedimentary environments. This tenet in addition to other germane diagenetic processes discussed in Section 5.1, will underpin the evaluation/interpretation of the porewater and column leach data.

5.4.2 Major Ion Chemistry of Tailings Porewaters

Porewater pH and electrical conductivity profiles measured for all sample sites (3, 4, 5, 6 and 9) are shown in Figures 5.34 and 5.35, respectively. In general, the porewater profile is vertically stratified in two distinctive geochemical zones:

1) An upper zone which extends from the surface of the tailings down to RL 35 m. This zone is characterised by high conductivity (> 25 mS/cm) and near neutral to slightly acidic pH water.

2) The lower zone which extends from the inflection point at RL 35 to the base of the dam. This zone is characterised by a 50% decrease in conductivity within a few metres of the inflection point and slightly basic pH water.

Like the overlying tailings pond water, the major ion chemistry is characterised by magnesium, sulfate, calcium, manganese, and ammonia as shown in Figures 5.36, 5.37, 5.38, 5.39 and 5.41, respectively.

Magnesium and sulfate are the dominant constituents comprising the bulk of the total dissolved solids (Figures 5.36 and 5.37, respectively). These ions maintain electrical neutrality and closely resemble the aforementioned conductivity profiles. Consequently there is a significant concentration gradient down the porewater profile with Mg and SO_4 concentrations in the upper zone peaking at 7500 mg/L and 35000 mg/L, respectively. Below RL 35 Mg and SO_4 sharply decline to 100 mg/L and 6000 mg/L, respectively.